EUROPEAN FUSION DEVELOPMENT AGREEMENT

EFDA–JET–PR(01)122

R.J. Buttery et al

Onset of Neoclassical Tearing Modes on JET

Onset of Neoclassical Tearing Modes on JET

R. J. Buttery, T. C. Hender, D. F. Howell, R. J. La Haye[1], O. Sauter[2], D Testa[3], and contributors to the EFDA-JET workprogramme*

Culham Science Centre, Abingdon, Oxon. OX14 3DB, UK.
[1]General Atomics, San Diego, USA.
[2]Centre de Recherches en Physique des Plasmas,
Association EURATOM-ConfÈdÈration Suisse, EPFL, 1015 Lausanne, Switzerland.
[3]Plasma Science and Fusion Center, Massachusetts Institute
of Technology, Cambridge, USA
** See annex of J. Pamela et al, "Overview of Recent JET Results and Future Perspectives", Fusion Energy 2000 (Proc. 18th Int. Conf. Sorrento, 2000), IAEA, Vienna (2001).*

Paper to be submitted for publication in Nuclear Fusion

ABSTRACT

A detailed study has been made of the onset and behaviour of (m=3, n=2) Neoclassical Tearing Modes (NTMs) on JET, validating many of the underlying concepts in NTM physics. In particular, fitting onset thresholds in terms of the correctly motivated physics parameters produces scalings closer to theoretical expectations. The use of such locally measured parameters also removes previous inconsistencies in the data between different divertor configurations. The evolution of island size with β, confirms the predicted levels of bootstrap current, and highlights the role of small island size stabilisation terms, which give rise to a seeding requirement for NTMs from some other instability. This seeding requirement is confirmed, and is generally provided by sawteeth in the cases studied here. However it appears doubtful that the seeds are induced by magnetic coupling in these cases. In particular the NTM always appears well below the n=2 sawtooth precursor harmonic frequency - although they often lock together once the NTM has grown close to saturation. Also, while plasma rotation profiles are favourable for a three wave interaction involving (4,3) and n=1 modes, irregular matches to the appropriate mode frequency condition appear coincidental, with no clear correlation between such matches, n=1 mode amplitudes, and (3,2) NTM growth rates. Thus other seeding models should be considered - we have discussed two possibilities: a temporary change to classical tearing stability due to the sawtooth;and flow variation leading to a change in ion polarisation current polarity. The full resolution of this issue is essential if a predictive theory of NTMs is to be obtained, but requires further more detailed experimental measurements, and development of the theoretical models. Finally, the nature of the (4,3) NTM hasalso been explored. This mode also requires a seed perturbation to be triggered (in these cases supplied by a sawtooth), and occurs at similar local parameter values as the 3,2 NTM, but with lower heating powers and β_N. A cascade process emerges in which successively lower mode number NTMs occur as β is raised.

1. INTRODUCTION

Neoclassical tearing modes (NTMs) are one of the critical issues for baseline scenarios in present and next step devices such as ITER. They reduce confinement in†'ELMy H-mode' plasma regimes (the main operating scenario envisaged for ITER) when the normalised plasma pressure, β_N [defined as the ratio of plasma thermal energy to magnetic field energy, normalised to the ratio I_p/aB_T, where I_p is the plasma current (MA); B_T, the toroidal field (Tesla); and a, the plasma minor radius (m)], is typically in the range 2-3 on present devices [1,2,3,4,5]. Simple empirical fits to data from various machines [5,6,7,8] show β thresholds for the modes scale in proportion to normalised Larmor radius, ρ_i^*, and hence thresholds might be expected to be lower on larger devices. However, the physics behind the onset mechanism for NTMs is complex, not only involving various stabilising terms, but also the process of seed formation (usually associated with some other form of instability) required to trigger the NTM. Recent physics based models [9] have shown that thresholds might be expected to rise as ρ_i^* falls to very low values (such as those anticipated for ITER), although predictions remain uncertain [10]. Therefore, it is a particular priority to identify and measure the

physical processes involved in mode onset, in order to validate our understanding, and the models used to predict scaling to larger devices.

NTMs arise when strong pressure gradients (with strong bootstrap currents) are present at low collisionality. They are metastable, requiring a 'seed' perturbation in order to be excited. The seeds must be induced by some other instability, most commonly sawteeth, but also fishbones, or possibly Edge Localised Modes (ELMs) [11]. On JET, the NTM manifests itself in various forms, most commonly as a (3,2) mode (denoting as poloidal, toroidal mode numbers: m,n) at intermediate β_N (~2–3) which degrades confinement (typically by ~20%), and can be disruptive at low q_{95} [12,10]. A more benign (4,3) NTM, which later decays away, is often observed prior to the (3,2) NTM. At higher β_N (≥3), a (2,1) NTM is usually observed leading to a severe loss of confinement, often with the plasma transitioning to L-mode and/or causing a current terminating disruption [4,5] or machine protection stop. In previous work on JET [5], the basic mode structure, confinement effects and threshold scaling of NTMs were described. This identified the modes as pressure (i.e. bootstrap) driven, with clear island structure, and therefore concluded that they are NTMs.

In this paper, results from further campaigns are reported, where special effort has been made to target fast data windows to the mode onset, and provide systematic scans in plasma parameters using standardised configurations and time histories. The regimes used are similar to those of Ref [5] - high β_N (~2-3) ELMy H-modes, and the NTM behaviour and identification (island structure, mode numbers, confinement effects, etc.) once the mode saturates in amplitude is similar to that reported previously. The main focus of this paper is to examine the nature of the seeding mechanism, and the role of the physics terms that govern NTM evolution and lead to the requirement of a seed perturbation. The behaviour of the (3,2) NTM is concentrated on, as it has a significant impact on confinement and a lower threshold in β_N than the more disruptive (2,1) NTM - and so is more accessible on JET. In section 2 a discussion of the basic underlying theory and importance of the seeding process is highlighted. The main experiments and their results are described in section 3, which examines the seeding process in detail, as well as the use of fitting models for onset criteria that are more closely based on the physics, the role of stabilisation terms in the mode evolution, and onset of higher (m,n) modes on JET. Conclusions, together with a discussion of key issues for next step devices and future directions of work required, are given in section 4.

2. BASIC THEORY AND EQUATIONS

2.1. MODIFIED RUTHERFORD EQUATION AND SMALL ISLAND SIZE EFFECTS

NTMs are driven by a helical region of reduced bootstrap current in a tokamak plasma. This arises as a result of pressure profile flattening in the region of an island, locally reducing the bootstrap current. Two effects have been proposed to oppose this for small island sizes. Firstly, long connection length compared to perpendicular distance across the island lead to incomplete pressure flattening inside the island [13]. Secondly ion polarisation effects [14] act to replace missing bootstrap in the island. These arise from E¥B drifts differing between electrons and ions (due to finite ion orbit

effects) in the region of the island: the ions see an average electric field over their banana orbits, while electrons (with much smaller orbit widths) see a more local effect. This leads to a net current when ion banana widths are comparable to the island size, which can be stabilising for the NTM. Consequently growth of an NTM requires a large enough seed island already present in the plasma. The seed must be generated by some other form of instability (most commonly this is a sawtooth) and so is thought to depend on further physical mechanisms governing the size of that instability, coupling to the NTM resonant surface, and shielding effects [15].

The physics of the NTM onset can be described by the modified Rutherford equation [16] for the evolution an island of size, *w:*

$$\frac{\tau_r}{r_s^2}\frac{dw}{dt} = \Delta' + a_{bs}\varepsilon^{1/2}\left(L_q / L_p\right)\frac{\beta_P}{w}\left(\frac{1}{1+w_d^2/w^2} - \frac{w_{pol}^2}{w^2}\right) \qquad (1)$$

This is expressed in terms of the tearing stability parameter (Δ'), bootstrap current ($a_{bs}\beta_p/w$ term), ion polarisation effect (w_{pol} term) and additional transport effects in the island (w_d term). β_p is the ratio of plasma pressure to poloidal magnetic field pressure at the NTM resonant surface. L_q and L_p are scale lengths for safety factor and pressure gradients respectively, ε measures the ratio of minor radius of the resonant surface, r_s, to its major radius. τ_r is the resistive time scale. Field curvature effects [17] have been omitted in this formalism, as they are expected to be modest at conventional aspect ratio (although are more significant in the spherical tokamak [18]), and shaping is held constant in the discharges discussed here. However, we note that recent work [19] has flagged another possible origin for the seeding requirement, with corrections to the field curvature term at small island size.

The ion polarisation term depends on whether trapped ions can resolve the island propagation timescales between collisions (or average over these timescales). It can be characterised using,

$$w_{pol} \approx \left[\, g(\nu,\varepsilon)\,(L_q/L_p)\,\varepsilon\,\right]^{0.5}\rho_{i\theta} \qquad (2a)$$

where 'g' is a function of normalised collisionality, $\nu=\nu_i/\varepsilon\omega_e^*$, with g=1 for ν<<1, and $g=\varepsilon^{-3/2}$ for ν>>1; ν_i is the ion collision frequency, ω_e^* is electron diamagnetic frequency, and $\rho_{i\theta}$ is the poloidal Larmor radius, all taken at the resonant surface. The constant of proportionality actually depends on plasma rotation [20] and is somewhat uncertain both experimentally and theoretically. The effects of incomplete pressure flattening depend on the ratio of perpendicular to parallel conductivities at the island. Various scalings are possible, dependent on the details of the transport model used and other assumptions. Some of these predict marginal neoclassical growth at island sizes much smaller than those expected from the data (as highlighted by Ref [6]). However by assuming convective transport (as adopted in Ref [9]), with flux limited parallel heat transport (as discussed in Ref [13]), larger values are obtained, with form:

$$w_d \approx \left[\chi_\perp R_0 L_q / v_e n_e\right]^{1/3} \qquad (2b)$$

where v_e is electron thermal velocity, n_e is electron density, R_0 is plasma major radius, and $\chi_\perp$ deduced from scaling laws such as ITER 93[21]. Finally it must be born in mind that for island widths comparable with the ion banana width, ion behaviour will be modified. This has already been pointed out for the ion polarisation current physics, where present models are only valid on scales much greater than $w_b \approx \varepsilon^{1/2}\rho_{i\theta}$. However at these island size scales the perturbation in the ion bootstrap current, which partly drives the NTM, may be reduced (although there will still be some drive from the electrons). Recent calculations [22] have shown that this can be significant for $w \sim 2\sqrt{7}w_b$. It enters into the modified Rutherford equation with similar form to that of finite island transport effects, and thus is capable of giving rise to an additional threshold for NTM onset.

Thus we see that NTM onset requires strong bootstrap currents (high β_p and low collisionality). Small island effects introduce further dependencies, for example on collisionality and poloidal (or toroidal) Larmor radius. The latter appears to account for the principal scaling of NTM onset threshold in β_N with machine size and toroidal field [10]. Variations in other terms, such as classical tearing stability or rotation, may also play a role.

2.2. DEPENDENCE OF NTM ONSET ON SEED AND OTHER PARAMETERS

If we rearrange Eq. (1) to yield the conditions for marginal growth of the NTM, given by dw/dt=0, we see this leads to the requirement of a critical seed of size, $w=w_{seed}$, for the NTM onset at a given β_p, thus defining $\beta_{p\text{-onset}}$:

$$\sqrt{\varepsilon}\left(\frac{L_q}{L_p}\right)\beta_{p\text{-onset}} = \frac{-r_s\Delta'}{a_{bs}}\cdot\frac{w_{seed}}{r_s}\Bigg/\left(\frac{1}{1+w_d^2/w_{seed}^2}-\frac{w_{pol}^2}{w_{seed}^2}\right) \qquad (3)$$

At small island sizes, the NTM can be stabilised completely by the w_d or w_{pol} terms, and $\beta_{p\text{-onset}}$ tends to infinity. If we neglect w_d for the time being, then we can define this seed size in terms of a ratio 'A', where $A = w_{seed}/w_{pol}$. Combining Eqs. (2a) and (3), the critical β_p for NTM growth is then given by:

$$\sqrt{\frac{L_q}{L_p}}\,\beta_{p\text{-onset}} = -r_s\Delta'\cdot\rho_{i\theta}^{*}\cdot\frac{A}{(1-1/A^2)}\cdot g(\nu,\varepsilon) \qquad (4)$$

where $\rho_{i\theta}^{*}=\rho_{i\theta}/r_s$. This effectively extracts the seed island size dependence of $\beta_{p\text{-onset}}$ in Eq (3), and is plotted in Figure 1 (solid curve). It is apparent that w_{pol} sets the scale for seed island size at mode onset. The lowest threshold in β_p (ie the marginal $\beta_p=\beta_{p\text{-marg}}$, below which an NTM cannot exist) occurs when $w_{seed}=\sqrt{3}w_{pol}$, with NTM thresholds rapidly rising as w_{seed}/w_{pol} falls below $\sqrt{3}$ towards 1. For seeds greater than this size, islands will move towards the 'saturation' line if β_p is high enough, or decay to zero size. For high β_p and $w_{seed}<\sqrt{3}w_{pol}$, once triggered, the mode will rapidly grow (as indicated by arrows in Figure 1) to saturation, such that Eq. (4) is satisfied for $A \rightarrow A' = w_{saturation}/w_{pol}$. Once saturated the mode's size will move up and down the right hand side of the curve according to the β_p value, only decaying away if β_p falls below $\beta_{p\text{-marg}}$. It should be noted that the ion polarisation model is only valid for $w >> \varepsilon^{1/2}\rho_{i\theta}$ (the ion banana width in the large aspect

ratio approximation). However, as shown later in this paper, w and w_{pol} are usually $>>\varepsilon^{1/2}\rho_{i\theta}$ on JET, and so this theory should be valid here.

At low collisionalities a strong part of the parametric dependency of the *lhs* of Eq. (4) will be on $\rho_{i\theta}^{*}$, with additional variation introduced due to changes in relative seed size (A), $r_s\Delta'$, profile changes and the collisionality function, g (at higher collisionalities). The typical trajectory of island size evolution with time during NTM onset on JET demonstrates island size rising rapidly after a sawtooth†'seed'; usually $\beta_{p\text{-}onset}>>\beta_{p\text{-}marg}$ (see section 3.6). This suggests the plasma is in the region where the threshold β_p for NTM growth is highly sensitive to the relative seed size. Any variation in the ratio w_{seed}/w_{pol} in JET experiments might therefore be expected to form a dominant part of any scaling of onset threshold in β_p.

It should also be borne in mind that island transport effects can be significant, particularly for larger devices [9], and will therefore raise thresholds even if ion polarisation currents are not sufficiently stabilising to prevent neoclassical growth. The form for this $\beta_{p\text{-}onset}$ dependence on relative seed island size in this case is also shown in Figure 1 (dashed curve). Here the minimum $\beta_{p\text{-}onset}$ occurs at $w_{seed}=w_d$, and $\beta_{p\text{-}onset}\rightarrow\infty$ as $w_{seed}\rightarrow 0$ (although field curvature effects may actually make this occur at finite island size [19]). The relevance of this model to present devices remains an issue of debate [6, 23].

The role of the small seed island terms is important in the extrapolation to larger devices, as they are predicted to lead to an upturn in NTM thresholds as $\rho_{i\theta}^{*}$ falls towards values expected for ITER [9]. This arises because the fall in island size predicted from a modelled seeding process, is faster than the predicted fall in small island size stabilisation effects. However, such upturns remain to be observed experimentally, as the low $\rho_{i\theta}^{*}$ at which this upturn is expected requires access to NTMs at higher currents or on larger* devices. Even if these upturns are present in deuterium plasmas, the fast particle stabilisation of sawteeth (anticipated in high fusion power plasmas) is likely to lead to larger sawtooth events, and thus larger NTM seeds and lower onset thresholds in β_N. Alpha particle stabilisation of sawteeth, leading to lower NTM thresholds, has now been observed directly on JET in Helium plasmas [24]. However, recent progress on sawtooth control with external current drive has also been promising, offering a tool to raise NTM onset β_N thresholds considerably [25], countering the alpha particle sawtooth stabilisation effects.

An important point to note in this discussion, is that the above considerations presume a seed is regularly generated, and that the modified Rutherford equation then determines whether this leads to neoclassical growth. However, the mechanism of this seed formation has not been resolved experimentally, and remains unclear - it is generally presumed that this occurs through some form of magnetic coupling [for example as used in Ref 9], and theoretical models have been constructed to explore this [15]. This should be explored, because if the seeding process is infrequent or can be inhibited in some way, then this provides additional means of mode avoidance.

Thus we see that it is important to explore the onset of NTMs, both from the perspective of the process that generates the seed, and the requirements from NTM theory that determine whether

such seeds grows to an NTM. This is crucial in understanding the onset behaviour and obtaining a predictive theory for NTMs. It is also important in specifying requirements for systems that might be required to control the NTM in future large devices.

3. THE EXPERIMENTS

Experiments were performed on JET in high β_N ELMy H-mode plasmas, with toroidal fields ~1-2T (to access high enough $\beta_N$levels with the available neutral beam heating power). Neutral beam heating was applied, usually with steadily increasing heating power levels in small steps (with timescales greater than typical sawtooth periods) to deduce marginal onset conditions. Densities were largely dictated by neutral beam fuelling, although massive gas puffing has been observed to have some effect. q_{95} values were maintained at ~3.4 to provide a good basis for comparison/ extrapolation to ITER, but avoiding locking of the (3,2) NTM and disruptions - which often occurs at lower q_{95} values [10]. Additional step-downs in NBI power were usually made at the end of the pulse, to observe the dependence of mode amplitude on β_p.

A typical pulse is shown in Figure 2. As β_N rises, a (4,3) mode is first observed, often associated with a slight reduction in the rate of rise of β_N as it saturates in amplitude. At higher β_N, sawtooth size tends to increase, and a (3,2) mode is observed. This causes a clear fall in confinement (typically ~15-20%), density often falls somewhat, plasma rotation falls, and the sawteeth become greatly reduced in size (although still present). As the (3,2) mode grows, the (4,3) mode decays away. Note that this pulse shows an interesting effect of self-healing from ~28s, with amplitude decreasing as β_N rises (see also Refs [25] and [26]). At low toroidal fields (1T), as in this pulse, continuation of heating leads to higher β_N ($\geq$3), destabilising a (2,1) mode. This has a catastrophic effect on confinement, triggering a transition to L-mode, stopping plasma rotation, and sometimes causing a disruption. The (2,1) mode is present for a time on locked mode detectors (no longer picked by the Mirnov coil measurements used for Figure 2), but decays away once β_N has fallen substantially.

In these experiments, care was taken to target fast magnetic and other data windows to capture the (3,2) mode onset and evolution as much as possible, so that the onset mechanisms, and critical parameters, could be studied in detail. Two fast data systems were used. The first of these allows up to 0.8s of (mainly 250kHz) fast data with poloidal and toroidal magnetic arrays, SXR and ECE diagnostics, plus a single 250kHz magnetics signal for the whole pulse. The second fast data system collects 4s of 1MHz data from 4 Mirnov coils in a toroidal array. Mode numbers are obtained by comparing phase differences between coils. Additional lower frequency response coils are interfaced to slower data acquisition systems in n=1 and n=2 combinations, for confirmation of toroidal mode numbers.

3.1. BEHAVIOUR AND IDENTIFICATION OF MODES

Observations of saturated (3,2) modes match those reported previously on JET [5], with clear island structures detected by ECE measurements in $\geq$1.7T pulses: typical displacements of temperature

contours in these experiments indicate saturated island widths ~10-15cm. Island sizes track the evolution of β_p, after initial rapid growth following first appearance. Islands remain present until the end of the last step of NBI power, when NBI and β levels are well below those at NTM onset. Although NBI levels at these final steps are typically 1/4 of NTM onset levels, β_N values are only ~40% lower than NTM onset values (as confinement improves at lower heating power). The hysteresis between onset and decay β values is expected from the underlying theory described in section 2.2, and is discussed further in section 3.6.

The (2,1) NTM remains present until β_N values have fallen to ~50% of onset levels. In one case (pulse 47295), where lower heating power is sustained (after triggering the mode at higher power) the NTM remains locked and exists at β_N values ~70% lower than onset levels (but will be partially error field driven once locked [27]).

A typical mode number plot at NTM onset is shown in Figure 3a for pulse 47285. Here the magnetic measurements identify an m=3 and n=2 structure for a mode commencing at 22.36s. This is clearly distinct from sawtooth harmonic and other mode activity. Later time-slices show this mode more emphatically, as it grows to saturation, dominating other mode activity. The second 1MHz toroidal magnetics array confirms the n number identification. The n=1 sawtooth precursor, has a high poloidal mode number due to toroidal coupling to rational surfaces (primarily q=3) further out in the plasma, which dominate the signal measured. A higher frequency n=3 mode is also observed, with m estimated from a poloidal magnetic array as between 4 and 5. The identification of higher poloidal mode numbers is non-trivial, as the local pitch angle of field lines depends on equilibrium details - the algorithm used in taken from Ref [28]. Typical errors in m are estimated to be ±1, and it is observed that magnetically estimated high m values tend to be systematically too high in these plasmas, when compared to estimates based on rotation and q profile information (see below). The (4,3) mode continues through the sawtooth crash, and is likely to be a (4,3) NTM - this is discussed further in section 3.7.

Toroidal rotation profile measurements (Figure 3b), confirm the m mode numbers: using the charge exchange diagnostic to locate the surface that is rotating at half the mode frequency (as it is n=2) gives a position in close agreement with the q=3/2 location from EFIT reconstructions. In other higher toroidal field pulses, EFIT mode locations have been confirmed against ECE measurements similar to those reported in Ref [5]. The higher frequency n=3 mode observed in Figure 3a is similarly identified with location between q=1 and q=1.5, and so m=4 (and not m=5 – which was possible from the magnetics alone). It should be noted that the rotation measured by charge exchange is that of the impurity species (carbon), and differs systematically from that of Deuterium [29]. However, specific calculations of this effect for these discharges show it to be at the ~5% level here, and it is therefore ignored.

These observations, together with those described in following sections (requirement for a seed, β tracking), and the similarity of regime and behaviour to that described in Ref [5], clearly identifies the (3,2) mode as an NTM.

3.2. CORRELATION OF (3,2) NTM ONSET WITH SAWTOOTH ACTIVITY

Examining the data underlying Figure 3a in more detail, we find the onset of the mode correlates with a peak in n=2 activity. This n=2 activity is identified as a non-linear harmonic of the sawtooth precursor activity, with exactly double its frequency, and well correlated with it. Through rotation profile measurements (Figure 3b), it is seen to be located near the centre of the plasma in the vicinity of the expected q=1 surface location. It is only clearly observable at high β_N values, where the sawteeth tend to be larger. In all measurable cases, the n=2 sawtooth precursor harmonics are clearly observed at the time of initial (3,2) NTM appearance and growth, and they occur at a *different* frequency to the (3,2) mode. This is a pattern reproduced in the wider data set, where mode numbers can be inferred by the comparability of pulses with direct mode measurements.

The correlation between sawtooth and NTM onset is investigated for a range of pulses in Figure 4. Here, NTM onset times are taken from spectrograms, sawtooth crashes from SXR measurements, and peak n=1 times from magnetic measurements. Correlation of NTM onset is better with peak n=1 activity, than with SXR crash. This is in accordance with an interpretation of the seed being magnetically driven by the sawtooth precursor (in particular its n=2 harmonic), for which the n=1 signal acts as a general indicator of size. When the crash is delayed with respect to peak n=1, the mode still forms at the time of peak n=1. This suggests that the correlation between the NTM onset and the sawtooth crash, arises simply because it is usually just before the crash that the precursor magnetic activity peaks. We explore this magnetic coupling hypothesis in more detail in the following sections.

After its initial appearance, the (3,2) mode frequency usually increases somewhat before reaching a distinct peak, after which frequencies of all modes slow. The peak in (3,2) mode frequency usually occurs as the n=2 sawtooth harmonic frequency locks to the (3,2) mode frequency (with the n=1 and n=2 sawtooth perturbation frequencies dropping slightly at this final locking stage). This locking although occurring soon after NTM onset, only happens after it has grown to significant size (several centimetres). Once locked in this way the modes remain locked throughout the whole time period of the NTM's existence in every case. The later general slowing of the plasma (also observed on the charge exchange diagnostic) and its accompanying modes, may be attributed to confinement degradation effects due to the NTM. In some cases where a sawtooth crash occurs after the (3,2) NTM onset, the crash event is associated with an increase in frequency and amplitude (and/or rate of growth) of the mode. This might be expected, as the crash event is associated with a transfer of particles and energy from inside to outside the q=1 surface - this could locally increase the pressure gradient that drives the growth of the NTM.

3.3. SEEDING PROCESS - MAGNETIC COUPLING HYPOTHESIS

A proposed mechanism for NTM seeding is via toroidal coupling of magnetic perturbations in the plasma to the NTM resonant surface. For example Ref [15] proposed coupling of n=2 sawtooth harmonics to the NTM. However, to induce such a response requires phase locking between the driving perturbation and the island being induced. Thus the absence of locking between the two

n=2 modes in Figure 3a is puzzling, indicating that this is not required to induce a seed. This absence of locking between the NTM and other perturbations at NTM onset has also been remarked upon on ASDEX Upgrade [11]. An extreme example from JET is shown in Figure 5a, where the (2,2) sawtooth harmonic, and a small (3,2) mode are observed to co-exist for over several hundred milliseconds. Again mode number identifications and frequencies are consistent with charge exchange data in Figure 5b. In this pulse, a large (3,2) NTM is only observed 2s later, re-excited after decay of the mode shown in Figure 5. Similar, though shorter lived, examples of dual n=2 modes can be observed in some other discharges (with the lower frequency n=2 usually growing directly to an NTM). Thus it appears that the initial formation of the island is very unlikely to result from strong coupling between the two n=2 modes. The later locking of these modes (discussed in section 3.1) indicates that toroidal coupling is indeed possible (and occurs), but requires the (3,2) mode to be of substantial size before an interaction can take place.

It has also been proposed that the seed island formation could occur through a non-linear 'three-wave' coupling process [30], involving (3,2), (4,3), and n=1 modes. These co-exist for a time during the initial growth phase of the (3,2) NTM in most of the discharges studied. The mechanisms for this non-linear interaction are discussed further in Ref [31], but to summarise: the basic concept is that the n=1 and n=3 modes combine to produce a beat perturbation with n=2 structure. The frequency of this beat perturbation would be equal to the difference of the n=1 and n=3 mode frequencies, giving rise to a frequency matching condition if this mechanism is to drive (3,2) island growth: $f_{3/2}=f_{4/3}-f_{n=1}$. An initial exploration of this showed that such a match does briefly occur in some cases. Indeed, the natural plasma rotation profiles lead to conditions in which such an interaction could occur: if we assume that mode frequency, f, is n times the bulk plasma toroidal rotation, ω (experimentally, this gives good consistency with charge exchange profiles), then the frequency matching condition can be regarded as a comparison of the q=4/3 toroidal rotation with a weighted average of q=1 and q=3/2 rotations: $3\omega_{4/3}=\omega_{n=1} + 2\omega_{3/2}$. It is trivial to show that for parabolic rotation and q profiles, and parameters similar to those of these plasmas, this condition would be expected to be satisfied exactly, while most other reasonably monotonic profiles would be expected to deviate by 1-2kHz at most.

We have explored the above frequency matching condition in detail, based on the observed magnetic perturbation frequencies for the 11 pulses from our experiments where the three modes clearly co-exist for a time. Two typical examples are shown in Figure 6. It can be seen that while for one pulse (47274), the frequency matching condition appears approximately consistent with non-linear coupling inducing the seed, in the other case (pulse 47275) the match is poor. This is the pattern observed throughout the data set. Only 6 of the 11 pulses exhibited an exact frequency match at time of (3,2) mode onset, with the other pulses exhibiting a 1–4kHz mismatch. Of the 10 pulses where the three modes co-existed for a significant period of time (at least 0.2s): 7 showed a frequency match over more than half the time period of co-existence, although deviating from this periodically; 3 were generally not well matched, disagreeing by 2–4 kHz. Also, although the (3,2)

NTM's first appearance itself usually coincided with a peak in magnetic activity (as discussed above), the subsequent growth rate of the (3,2) island did not correlate at all well with n=1 amplitude (the supposed main driving perturbation) - this is again apparent in Figure 6. Finally, in at least two other discharges from the series, either the n=1 or the (4,3) modes were completely absent during the initial growth of the (3,2) mode. The similarity in general phenomenology of these cases to the other discharges, and amongst the whole series of discharges generally, makes it hard to argue that different seeding mechanisms are taking place in different discharges. Thus while theoretical considerations, and experimental profiles, suggest a three-wave coupling might easily take place in such discharges, the lack of correlation between the frequency matching, n=1 amplitude, and (3,2) growth rate suggests that this is not the dominant process in the majority of these discharges.

A further problem with the three wave model is the recent suggestion [32], and subsequent observation, that harmonics non-resonant with the (3,2) NTM, such as those from the (4,3), can have a stabilising effect on a (3,2) island. This has been observed on ASDEX Upgrade and JET [25,26], where substantial confinement recoveries were observed following appearance of intermittent (4,3) modes at high β values [33]. Indeed it appears likely that this effect is playing a role towards the end of the discharge in section†3.6, and an exceptionally clear example is described and modelled in Ref [34]. Thus any three wave coupling model must also explain why this apparently strongly stabilising non-resonant effect is not present during (3,2) NTM onset.

3.4. SEEDING PROCESS - OTHER CONSIDERATIONS

The above discussion leaves the mechanism of the seeding process uncertain in these discharges, casting doubt on two obvious possibilities via magnetic coupling, despite the clear correlation on NTM onset time with sawteeth established in section 3.2. A key question is: at what point is the (3,2) mode growth "neoclassical" in origin? (i.e. governed by Eq. (1) with a negative Δ'). Also: how does the (3,2) growth relate to sawtooth precursor activity? To explore these questions further we examine the sizes of islands left in the plasma at the end of the strong n=1 sawtooth precursor activity - notionally the end of the seeding process, if the precursor activity is driving the seeding. The island size taken is that during the last period of marginal growth at the end of the sawtooth precursor phase (where amplitude is either flat or keeps returning to a minimum level - additional excursions may originate from sawtooth precursor harmonics). A typical such measurement is shown in Figure 7, where we see that the growth of the (3,2) NTM coincides with strong sawtooth precursor activity until 20.42s. Island sizes are obtained by mapping back to the perturbation at the resonant surface using:

$$\left|\tilde{B}_r\right| = \frac{1}{2}\left(\frac{b}{r_s}\right)^4 \left|\tilde{B}_\theta\right|_{wall} \qquad \text{and} \qquad w_{seed} \approx \left(\frac{16 r_s R_0 \left|\tilde{B}_r\right|}{3 s B_{\phi 0}}\right)^{1/2},$$

where b is the minor radius of the poloidal field perturbation detector, $\left|\tilde{B}_\theta\right|_{wall}$ is the perturbation amplitude measured at the detector, and s is the magnetic shear. This is based on a cylindrical approximation, and so we have calibrated such estimates against ECE measurements of island size by introducing an additional factor of 0.6 on island size.

The resulting island sizes at the end of the sawtooth precursor phase are shown in Figure 8 for 12 pulses, plotted against local drive for the NTM $[(\varepsilon L_q/L_p)^{0.5}\beta_p]$ from the *lhs* of Eqn. (3). Here we see that these sizes are much larger than the scale lengths associated with small island size stabilisation effects discussed in section 2. Recall that these predicted a minimum $\beta_{p\text{-}onset}$ (i.e. $=\beta_{p\text{-}marg}$) at either $w_{seed}=\sqrt{3}w_{pol}$, w_d, or $2\sqrt{7}w_b$ (dependent on which model is dominant). Figure 8 shows that the island sizes are either greater than or comparable to these scales. Note that here $\beta_{p\text{-}onset}>>\beta_{p\text{-}marg}$ (as discussed in section 3.6). Thus we conclude that at the end of the sawtooth precursor phase, the mode must have already been growing neoclassically for some time, as it has reached large size and β_p is much greater than $\beta_{p\text{-}marg}$. Therefore, if the n=1 precursor activity were the main drive for the NTM formation, then we would have expected earlier (and weaker) sawtooth precursors to trigger the NTM at lower β_p.

Exploring this further, spectrograms of magnetic signals for each discharge show that in most cases there is no coherent (3,2) mode whatsoever before that which grows to an NTM. This is examined in more detail in Figure 9 where for 16 discharges we plot peak magnetic perturbation amplitude in the (3,2) NTM frequency range, square-rooted and calibrated to produce equivalent (3,2) island size. Recall that from Figure 8 all NTMs are left at a size in the range of 5 to 8cm at the end of the sawtooth precursor activity. If the required seed size for marginal neoclassical growth were in this range (despite the high $\beta_p>>\beta_{p\text{-}marg}$), then one would expect smaller decaying seeds to be observed earlier. However, in all cases in Figure 9, we see that prior to the NTM onset, the magnetic perturbation amplitude stays well below 3cm (indicated by the dotted lines for each pulse). A possible explanation of this would be that the seed required for neoclassical growth is quite small. But if this were the case, and the sawtooth precursor is driving the mode, then why did it take such large sawtooth precursors (which exist up to island sizes of several cm) before the NTM appears? Why did not earlier sawtooth precursors trigger the NTM?

The experimental evidence points away from the concept of seeding via magnetic coupling, and suggests some other aspect of the sawtooth behaviour leads to formation of an island large enough to grow neoclassically. Recalling the correlation between NTM onset and the sawtooth, a possible alternative model for NTM seeding can be conceived. It appears that the seed is being generated at some 'natural' frequency of the q=3/2 surface (not locked to other perturbations or beat frequencies). This suggests that rather than being induced by some additional physics to the modified Rutherford equation (1) (such as magnetic coupling), it may be originating due to changes in one or more terms of the equation, leading to positive growth rates for islands with small amplitude. Once the mode reaches large amplitude the expected toroidal coupling process can take place, and indeed an exact locking between (3,2) and (2,2) perturbations is nearly always observed once at large island size. This explains the observed frequency rise that usually occurs during the initial growth phase of the mode. Once the (2,2) and (3,2) perturbations lock, the confinement reducing effects of the mode lead to the observed slowing of the whole plasma - a pattern that is evident in all of the discharges in the study. But what induces the initial tearing?

One possibility is that the sawtooth induces a *temporary* change in classical tearing stability (Δ'), due to redistribution of current from inside to outside the q=1 surface. This would be likely to increase current gradients at q=3/2 and thus classical tearing instability, leading to formation of an island. This is an extension of the models proposed by Refs [35] and [36], where (apparently triggerless) NTMs were shown to grow out of conventional tearing modes in TCV discharges. As the island grows to large amplitude, neoclassical growth would be expected to take over (and Δ' to fall as a result of the large island size), consistent with the modelling in section 3.6. This possibility is backed by indicative modelling using JET-like equilibria and moving a 'bump' in the current profile from the core to off-axis to raise q_0 from below to above 1 (while minimising other changes to current profile). For a range of possible pre- and post- crash profiles the (3,2) classical tearing stability, Δ'_{32} (calculated in the cylindrical approximation) was always observed to rise significantly, and more with larger rises in q_0. (Such a dependence of Δ'_{32} with q_0 was also predicted in Ref [37]). It is possible that the development of a negative Δ'_{32} is contributed to by the neutral beam effects on the current profile. However, a principal difficulty with such a model is the observation that in many cases the (3,2) mode starts its growth slightly before (eg Figure 3) or between sawtooth crashes. Possibly this might be associated with a prior sawtooth changing the Δ', but clearly the model requires theoretical development before conclusions can be made. It also requires more detailed measurements (eg of current profiles with MSE) - this will be studied in future experiments on JET.

We should note that a Δ' based seeding model favours finite island transport effects as the dominant mechanism governing the requirement for a seed to trigger the NTM. Ion polarisation current effects would be expected to stabilise Δ' driven modes, whereas finite island transport effects can only enter once the island is dominantly bootstrap driven. Ion polarisation current effects could be suppressed if island rotation was zero in the E×B=0 frame of reference [20] (it has not yet been possible to measure this on JET with sufficient accuracy).

Considering the role of rotation and ion polarisation effects raises another possible mechanism for NTM seeding: incremental changes in rotation profiles, which have been observed to respond to sawteeth in the time leading up to NTM onset [38], might lead to a reversal in MHD fluid rotation in the E×B=0 frame of reference, and thus in the polarity of the ion polarisation current term. This could lead to the ion polarisation currents directly driving the initial formation of the NTM. Further changes in flow profiles as the island grows mean that ion polarisation current effects might even change further during the mode evolution (eg from destabilising to stabilising) to explain later evolution and mode decay. However, much more detailed measurements are required to resolve the direction of rotation of the island in the ExB=0 frame, and explore this question in more detail.

To summarise, we see that in general the data does not appear to favour magnetic coupling models of seed island formation in these discharges. The most serious problem with these models is the lack of correlation between the frequencies of the various modes involved. We have suggested some alternative models. These require extensive further experimental investigations with additional measurements, and formulation of more detailed theoretical models, possibly along the lines indicated

above. However, a key problem remains in explaining why we rarely see decaying seeds before the NTM. It seems that in most cases, once a seed of any sort is produced, it leads to an NTM (with the exception of one or two brief examples of transient modes). It also remains difficult to explain why the initial appearance of the mode appears better correlated with peak MHD activity (consistent with the mode coupling causing seeding), rather than the crash event itself.

3.5. PROFILE EFFECTS AND ROLE OF 'PHYSICS' PARAMETERS

In previous work on JET, NTM thresholds have been quoted in terms of global plasma parameters, most commonly β_N. This is a sensible approach for extrapolation to next step devices, where profiles are somewhat uncertain, so we assume similarity with a present device's plasmas. However, as discussed in section 2, NTM onset actually depends on local parameters at the rational surface, and so will be sensitive to changes in plasma profiles. Thus a comparison between data for NTM onset from different divertor configurations (the 'Mark IIa' and 'Gas box' divertors) on JET reveals a systematic difference in thresholds in β_N. Plotting β_N at NTM onset against normalised toroidal Larmor radius, $\rho_{i\phi}^*$, (Figure 10a), we see that thresholds are significantly lower for the MkIIA divertor configuration. Here we are adopting the definitions of Ref [9] (and section 2) for β_N, ν, and $\rho_{i\phi}^* \equiv \rho_{i*}$, as used for inter-device scaling. These are reasonable choices when the dependence is explored in terms of global parameters, assuming similar profiles across the scan. Performing a logarithmic regression fit of β_N to these parameters, we find that in order to minimise scatter, the Mark IIa divertor data must have β_N thresholds scaled upwards by 19%. Applying this scaling then raises the coefficient of determination in the fit, r_2, from 29% to 50%, to obtain:

$$\beta_N = 95.5\ \rho_{i\phi}^{*\,0.71\pm0.14}$$

The collisionality scaling in this fit is forced to zero, as a fit in two dimensions yields an index for ν of -0.02 ± 0.03 (zero dependence within error bars). This differs slightly from previous studies on JET [5], which adopted a definition of collisionality based on more global variables, without ion temperature or pressure gradient terms (our approach increases statistical errors somewhat, but is more closely related to the underlying physics set out in section 2). The $\rho_{i\phi}^*$ scaling of the individual data sets ('Mark IIa' and 'Gas box') are consistent with each other, and with the combined data set, within error bars.

However, if we plot thresholds in terms of the relevant *local* plasma parameters (where $\beta_p = 2\mu_0 P_{q=1.5}/B_p^2$, based on a local pressure value and line average poloidal field at the resonant surface) that appear in the onset equation (3), as shown in Figure 10b (with correction for collisionality variation using the fit below), we see that the offset between different divertors is removed. This validates the approach used in the theoretical models discussed in section 2, indicating that the local parameters used are the ones that govern behaviour. Further checks have confirmed that the best fits are obtained with the appropriate profile factors included. The most significant contribution to the differences between these two approaches comes from differences in the pressure profile. This can be seen in Figure 11 which shows that in the Mark IIa divertor configuration, the ratio of

local plasma pressures at the q=1.5 surface (used in β_p) to volume average pressure (used in β_N) was systematically higher, increasing NTM drives for a given β_N, and thus expected to lower thresholds in terms of β_N, as observed.

A regression fit in the relevant local physics parameters used in section 2 gives:

$$(L_q/L_p)^{0.5}\beta_p = 16.2\ \rho_{i\theta}^{*\,1.11\pm0.21}\ \nu^{-0.14\pm0.07}$$

It is worth noting that despite the increased statistical error likely in the local parameter approach (due to many more noisy local measurements required), the correlation between fit and data is much improved over all the β_N fits, with the coefficient of determination, r_2, reaching 88%.

Comparing this fit with equation (3) we see that this is very close to the theoretically predicted form based on the ion polarisation model in section 2.2. At face value this would indicate that the effects of other terms, such as variation in Δ' or relative island size, A, are small or cancel out. The JET plasmas appear to lie well into the collisionless regime, where $g(\nu)$=1 (as expected from the calculated values for ν, which are <<1). However, the model described in section 2 presumes a regular seeding event (leading to an island which may then decay or grow, according to the modified Rutherford equation). As outlined in section 3.4, this does not appear to be a feature of the experimental data, where once a suitable mode appears, it usually grows to an NTM. Until the seeding process is fully resolved, both experimentally and theoretically, such comparisons of scalings should be treated with a degree of caution.

In summary, we see that application of a physically motivated model of NTM onset behaviour explains systematic offsets in the data, improves fits, and demonstrates a good match between observed behaviour, and that expected from theory. We note that this is also consistent with possible scalings recently obtained for the finite island transport model, which can scale as $\beta_N \sim \rho^* \nu^{1/2}$ [39]. This gives a degree of confidence that the physics models at least contain many of the right ingredients, and appear to be a reasonable representation of reality. However, we note that from section 3.3, that until the seeding process is resolved, the form obtained here cannot represent the complete story regarding NTM onset behaviour.

3.6. ROLE OF ION POLARISATION/TRANSPORT TERMS IN MODE EVOLUTION

In Ref [5], the pressure driven nature of the NTM was confirmed by mode amplitude tracking in β_p. In the campaign reported here, pulses with large step-downs in heating were programmed in order to examine the role of the other terms in the island evolution. The step down in heating reduces β_p and island size to levels close to the onset thresholds, where ion polarisation or island transport effects are predicted to help stabilise the mode - so their effects should be visible. The data for island size evolution (n=2 amplitude) is fitted to the modified Rutherford equation for pulse 47276, where ECE measurements provide an estimate of saturated island sizes. The exact form used for the fit is:

thus defining $a_{bs}' - a_{GGJ} = a_{bs}\,\varepsilon^{1/2}\,(L_q/L_p)$, and $a_{pol} = w_{pol}^{\,2}\,a_{bs}\,\varepsilon^{1/2}\,L_q/L_p$ in terms of Eq. (1). A term for field curvature effects [40] has been inserted, a_{GGJ}, which is calculated from the equilibria [41]. Fits were performed with three different constraints: no ion polarisation or island transport terms (a_{pol}=0, w_d=0); ion polarisation but no island transport term (w_d=0); island transport but no ion polarisation term (a_{pol}=0). $r_s\Delta' = -m$ (a reasonable† 'guess') is assumed, and the bootstrap coefficient is adjusted to approximately match island size, which is taken to match measured values from ECE (~10cm) during the high β_p region (19-20.5s). The results should be taken as indicative, as changing $r_s\Delta'$ will change the detailed behaviour of the fits. However, this clearly shows (see Figure 12a) that only by including terms from ion polarisation or island transport effects, can the fall in island size with β_p be reproduced, although neither are a perfect match at small island sizes. These effects have a stabilising influence on the NTM, and thus reduce the anticipated island size at low β_p, ultimately removing it entirely. We also note that in the last 0.8 of the mode's existence (26.1 to 26.9s) the mode spontaneously reduces in size to a level well below that predicted by the models. This coincides exactly with the appearance of an n=3 mode, and may be related to the stabilising effect proposed due to a different helicity perturbation acting on a magnetic island [32]. A further, clearer example of this effect is explored in Ref [34].

Curves of growth rate vs island size are shown inFigure 12b for the three fits obtained, where plots are given for β_p=0.5 and 0.9. When compared with the upper plot (no stabilising terms), the middle and lower plots show the role of the two stabilising terms, which lead to requirements for seeds ~2–5cm in width (dependent on model and β_p) to trigger neoclassical growth. From Figure 12a we see that both have similar impacts on the island size as β_p falls. The marginal β_p, $\beta_{p\text{-}marg}$, below which an NTM cannot exist is just above 0.5 for both models. However, critical seed sizes for positive NTM growth at high β_p are much smaller for the island transport model (middle plot of Figure 12b) - even small seeds can trigger NTMs with this model, provided β_p is high enough.

The fit parameters are compared with theoretical expectations (based on formulae from Ref [16] and experimental parameters) in Table 1. $r_s\Delta' = -3$ is typical for toroidal plasma, and the bootstrap term appears consistent with fits; field curvature effects are weak. The ion polarisation current term has had to be increased, compared to theoretical expectations. However we note that both of the small island size stabilisation terms have uncertainties: with regard to plasma rotation (for ion polarisation effects) and choice of transport model (for finite island transport effects). Finally, resistive timescales have had to be considerably shortened. However, a wider examination of NTM evolutions in JET discharges [34] has shown this not to always be the case, and such discrepancies can largely be accommodated by a different choice for Δ'.

3.7. ONSET OF 4,3 NTMS

Studies have also explored the onset of the (4,3) NTM on JET. An example where fast data was able to capture the onset is shown in Figure 13, where the mode is excited during an interval of particularly large sawtooth precursor activity. Checks based on rotation and safety factor profiles indicate that such modes must be coming from a surface between q=1 and 1.5 (see for example Figure 3b and

Figure 5b), and so is identified as m=4. As with the (3,2) NTM onset, a higher number mode is seen prior to the (4,3) onset (5,4 in this case), which peters out once the (4,3) grows. Thus the picture emerges of a cascade of modes as heating power is raised: first (5,4) then (4,3), (3,2), and finally (2,1), each having progressively worse effects on the plasma. This ordering may be related to the surfaces closest to the q=1 being affected more easily by the triggering instability, and so having NTMs triggered more readily (at lower β). It is possible that the observed decay of one mode following appearance of another with different helicity may be related to the stabilising effect proposed due to a different helicity perturbation acting on a magnetic island [32]. Alternatively the lower mode number island may degrade confinement within its rational surface radius, thus reducing the drive for the higher number mode, making it sub-critical for neoclassical growth, and thus explaining its disappearance.

As for the (3,2) NTM, there is a strong correlation between (4,3) NTM onset and sawtooth activity, indicating a seeding role for the sawtooth. This is illustrated in Figure 14, where we see that the NTM onset (as measured by its first appearance on spectrograms) usually occurs within one third of a sawtooth period relative to peak magnetic amplitude associated with sawtooth precursor, or soft X ray crash.

The (4,3) modes usually appear well before onset of a (3,2) NTM on JET, generally having a significantly lower neutral beam power threshold. However, the threshold in β_N for the (3,2) NTM is only on average 8% higher than that for the (4,3) mode in this set of discharges (and in some cases, the 3,2 NTM has a lower β_N threshold than the 4,3). This is possibly related to the confinement reducing effect of the (4,3) island in the plasma, as can be seen in Figure 2, where the rate of rise in β_N is observed to fall markedly at the time of (4,3) NTM onset. When this is explored in local parameters, a much larger rise, averaging 35%, is observed in the drive (at the q=3/2 surface) for the (3,2) NTM $[(L_q/L_p)^{0.5}\beta_p]$ between times of (4,3) and (3,2) mode onset. Thus following (4,3) NTM onset, profiles are continuing to steepen in the region of the q=1.5 surface in the plasma (as heating power is increased), while confinement is degraded nearer the core of the plasma due to the (4,3) island.

If we examine the thresholds in terms of the local drives for the NTM, calculated at q=4/3 for the (4,3) but at q=3/2 for the (3,2) mode, we observe that the thresholds are similar in magnitude. This is shown in Figure 15, where thresholds are corrected for collisionality variation using the appropriate fits to data. This similarity in thresholds is somewhat surprising, as coefficients in the model (for example Δ', coefficients in the ion polarisation term, and seed island produced) might be expected to vary with rational surface shape and mode numbers. A regression fit to the scaling for the (4,3) NTM onset yields:

$$(L_q/L_p)^{0.5}\beta_p = 52.2\ \rho_i\ {}_\theta^{*\,1.60\pm0.13}\ \nu^{-0.15\pm0.06}$$

The weak collisionality scaling is very similar to the (3,2) NTM. However, the dependence on normalised poloidal Larmor radius is considerably steeper than for the (3,2) NTM. This may indicate either a dependence of relative island size or Δ' on β_p in equation (3). Nevertheless, it shows that scalings can change for different modes.

4. CONCLUSIONS

To conclude, we have explored the onset of (3,2) neoclassical tearing modes on JET, comparing it with theoretically expected forms of behaviour, identifying scalings and key physics effects. The data to achieve this has been obtained by targeting fast data windows to the onset of the mode, with systematic scans in various plasma parameters (in otherwise uniform configurations), and heating power slowly ramped up to provide plasmas in conditions marginal for NTM onset.

We find that the general behaviour of the (3,2) NTM is reasonably well described by the theory. The onset threshold scaling is most consistently represented in terms of locally measured parameters used in the underlying theory. This removes previous inconsistencies in the data, and parameters are close to their theoretically expected values. Modelling of discharge evolutions confirms the requirement for small island size stabilisation terms, such as ion polarisation current or incomplete pressure flattening in the vicinity of the island. These effects give rise to the need for a seed island (originating from some other source) to trigger the NTM. The modelling shows that either or both effects are capable of explaining island size evolution.

There is clear evidence for a seeding process associated with other instabilities in the plasma, with strong time correlations between NTM onset and sawtooth precursor mode amplitude. However, the lack of a reproducible frequency match between the (3,2) NTM and other modes in the plasma (such as sawtooth precursor harmonics and/or beating with 4,3 modes) suggests the production of the seed island is not through magnetic coupling, as has been proposed previously [9,15,30]. In particular, the most obvious form of this, via toroidal coupling to the n=2 harmonic of the sawtooth precursor [15] is rejected; the mode is always born well below the (2,2) sawtooth precursor harmonic frequency, only accelerating up to this frequency once the (3,2) has grown to substantial size, well above the expected scales for marginal neoclassical growth. In addition, while plasma rotation profiles are favourable for a three wave interaction involving (4,3) and n=1 modes, irregular frequency matches to the appropriate condition appear coincidental, with no clear correlation between the condition, n=1 mode amplitude and (3,2) NTM growth rate. Indeed in some cases the three modes are not present simultaneously at all, rejecting the three-wave hypothesis outright in these cases. In general, it seems that the (3,2) mode is born at some natural frequency, with coupling (to the n=2 mode) only coming into play once it has reached substantial size.

An alternative explanation of the seeding may lie in a classical tearing trigger, arising from temporary profile changes associated with the sawtooth event, although this still has problems with cases where the NTM is initiated ahead of the sawtooth crash. Another hypothesis is that changes to flow profiles may alter the polarity of ion polarisation currents, making them destabilising. We have briefly discussed these, but the full resolution of the seeding issue requires further, more subtle, experimental measurements, together with the formulation of more detailed and quantitative theoretical models to allow comparison against data. Thus the seeding issue remains an open question. It is even possible that with the plasma metastable to NTMs, a variety of seeding mechanisms could play a role, dependent on circumstance, although the similarity of phenomenology between discharges discussed in this paper makes this appear unlikely here.

Scalings for the onset of the (4,3) NTM have also been obtained. This mode also requires a seed perturbation to be triggered (from a sawtooth in these cases). Thresholds in terms of the underlying physics parameters (at the q=4/3 surface) are similar to values (at q=3/2) for the (3,2) NTM. The (4,3) modes occur at only slightly lower β_N, than the (3,2) NTM, although local bootstrap current drives at q=3/2 strengthen considerably between (4,3) and (3,2) mode onset, indicating an effect of the (4,3) on plasma pressure profiles. The coefficients of the scalings for the (4,3) NTM onset differ from the (3,2) NTM indicating that the physics can change between different modes. The modes appear to be suppressed by large (3,2) NTMs, and a cascade process seems to be emerging with more benign higher mode number NTMs observed at low β_N, but progressively more serious, lower mode number NTMs being triggered as β_N rises, and the higher number modes decaying away.

These results raise a number of issues for the future. Although many of the aspects of NTM physics are validated by observations on JET, the process by which NTMs are triggered remains a critical uncertainty, with traditional magnetic coupling mechanisms looking unlikely to be appropriate for many of the discharges explored here. Thus, considerable further effort is required to resolve the physics understanding of this process, and provide a predictive theory. In particular, further experimental measurements must be taken to test new seeding models, and more detailed development of such models is required to provide a quantitative theory. In addition, more detailed studies of island evolution will help discriminate between (and constrain/verify the form of) ion polarisation current and finite island transport models, which may scale differently when extrapolated toward burning plasma devices. The development of the ion polarisation current model to small island size scales is also desirable in understanding NTM onset, and fitting behaviour. Overall the good progress being made experimentally, together with the developing theoretical framework, provides good grounds for optimism that these issues will be resolved.

ACKNOWLEDGEMENTS

This work was partially funded by the UK Dept. of Trade and Industry, and EURATOM. It was conducted partly in the framework of the JET Joint Undertaking, and partly under the European Fusion Development Agreement. Olivier Sauter was supported in part by the Swiss National Science Foundation. Robert J. La Haye was supported by U.S. Department of Energy Contract No. DE-AC03-99ER54463.

REFERENCES

[1] CHANG, Z., et al., Phys. Rev. Lett. **74** (1995) 4663.

[2] GATES, D. A., et al., Nucl. Fus. **37** (1997) 1593.

[3] GATES, D. A. et al., Contr. Fus. and Plas. Phys. (Proc. 22nd Eur. Conf. Bournemouth, 1995), Vol. 19C, European Physical Society, Geneva (1995) 117.

[4] LA HAYE, R. et al., Nucl. Fus **37** (1997) 397.

[5] HUYSMANS, G. T. A., et al., Nucl. Fus. **39** (1999) 1965.

[6] LA HAYE, R. J., SAUTER, O., Nucl. Fus. **38** (1998) 987.

[7] G‹NTER, S., et al., Nucl. Fus. **38** (1998) 1431.

[8] G‹NTER, S., et al., Plasma Phys. Control. Fusion **41** (1999) B231.
[9] LA HAYE, R. J., et al., Phys. Plas. **7** (2000) 3349.
[10] BUTTERY, R. J., et al., Plasma Phys. Control. Fusion **42** (2000) B61.
[11] GUDE, A., et al., Nucl. Fus. **39** (1999) 127.
[12] GRUBER, O., et al., Fusion Energy (Proc. 16th IAEA, Montreal, 1996) **1** (1997) 359.
[13] FITZPATRICK, R. et al. Phys. Plasmas **2** (1995) 825.
[14] WILSON, H. R., et al., Phys. Plasmas **3** (1996) 248.
[15] HEGNA, C. C., CALLEN, J. D., and LA HAYE, R. J., Phys. Plas. **6** (1999) 130.
[16] SAUTER, O., et al., Phys. Plas. **4** (1997) 1654.
[17] GLASSER, A. H., GREENE, J. M., JOHNSON, J. L., Phys. Fluids **18** (1975) 875.
[18] BUTTERY, R. J., et al., **88** Phys. Rev. Lett. (2002) 125005.
[19] LUTJENS, H., et al., Phys. Plasmas **8** (2001) 4267.
[20] WILSON, H. R., et al., Plas. Phys and Contr. Fus. **38** (1996) A149.
[21] ROSENBLUTH, M., et al., Plas. Phys. Contr. Nucl. Fus. Res. (Proc. 15th IAEA, Seville, 1994) **2** (1995) 517.
[22] POLI, E., et al., Phys. Rev. Lett. **88** (2002) 075001.
[23] ZOHM, H. et al., Phys. Plasmas **8** (2001) 2009.
[24] M. MANTSINEN et al., Phys. Rev. Lett. **88** (2002) 105002.
[25] SAUTER, O., et al., Phys. Rev. Lett. **88** (2002) 105001.
[26] GUNTER, S., GUDE, A., MARASCHEK, M., Phys. Rev. Lett. **87** (2001) 275001.
[27] BUTTERY, R. J., et al., Nucl. Fus. **40** (2000) 807.
[28] SMEULDERS, P., et al., Plas. Phys. Control. Fus. **41** (1999) 1303.
[29] TESTA, D., et al., Phys. Plas. **9** (2002) 243.
[30] NAVE, M. F. F., LAZARRO, E, et al., Contr. Fus. Plas. Phys. **24B** (Proc. 27th EPS, Budapest, 2000) 1100 (and [31] below).
[31] NAVE, M. F. F., et al., "Triggering of neo-classical tearing modes by mode coupling" submitted to Nucl. Fus.
[32] YU, Q., G‹NTER, S., LACKNER, K., Phys. Rev. Lett. **85** (2000) 2949.
[33] G‹NTER, S., et al., Contr. Fus. Plas. Phys. **25A** (Proc. 28th EPS, Funchal, 2001) 2149.
[34] SAUTER, O., et al, "Marginal beta limit for neoclassical Tearing Modes in JET H-mode discharges", submitted to Plas. Phys and Control. Fus., 2002.
[35] REIMERDES, H. et al., Phys. Rev. Lett. **88** (2002) 105005.
[36] BRENNAN, D., et al., General Atomics report GA-A23768, submitted to Phys. Plas. (2002).
[37] CARRERAS, B. et al., Phys. Fluids **23** (1980) 1811.
[38] BUTTERY, R. J. et al., Contr. Fus. Plas. Phys. **25A** (Proc. 28th EPS, Funchal, 2001) 1813.
[39] ZOHM, H., et al., Phys. Plas. **8** (2001) 2009.
[40] KOTSCHENREUTHER, M., HAZELTINE, R. D., MORRISON, P. J., Phys. Fluids **28** (1985) 294.
[41] LUTJENS, H. et al., Comput. Phys. Commun. **97** (1996) 219.

Quantity	Theory	Fit: $w_d = 0$	Fit: $a_{pol} = 0$	Fit:$a_{pol} = 0$, $w_d = 0$
$r_s\Delta'$	−3	−3 (fixed)	−3 (fixed)	−3 (fixed)
a_{bs}	0.8	0.75	0.79	0.73
a_{GGJ}	−0.1	−0.1 (fixed)	−0.1 (fixed)	−0.1 (fixed)
a_{pol} (cm^2)	$-1.5cm^2$	$-4cm^2$	0 (fixed)	0 (fixed)
w_d (cm)	1−3cm*	0 (fixed)	3.1cm	0 (fixed)
τ_r(s)	10	3.4	3.4	3.4

*dependent on transport model assumed

TABLE 1: Comparison of theoretical and fitted parameters for island evolution in pulse 47276.

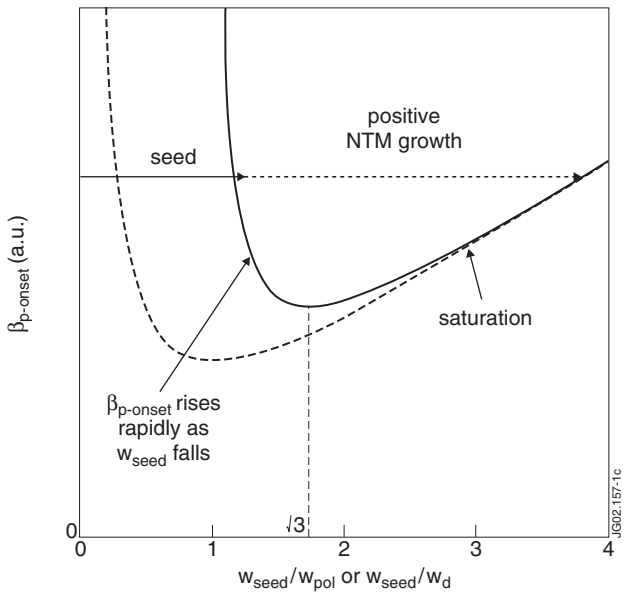

Figure 1: Dependence of $\beta_{p\text{-onset}}$ on w_{seed} in Eq. (3) (holding all other quantities constant) if either ion polarisation (solid) or finite island transport (dashed) models dominate.

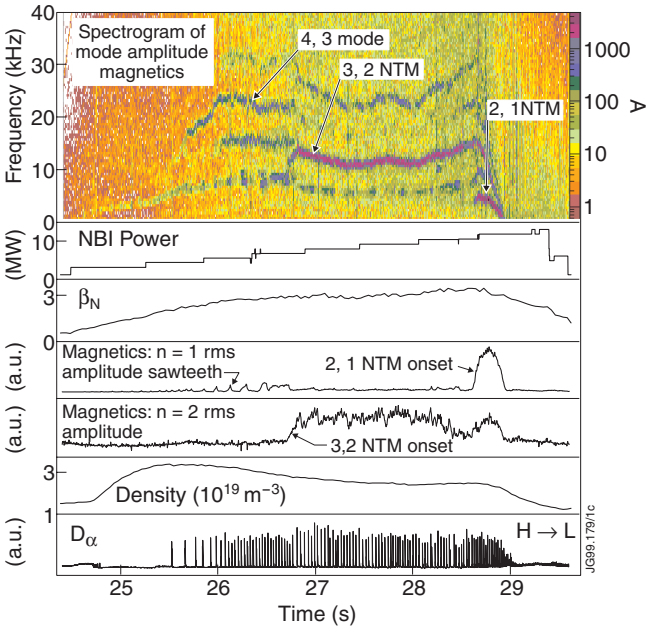

Figure 2: Typical example of a neutral beam heated pulse (47296) in which NBI power is steadily increased, causing a rise in β_N. Spectrogram distinguishes various modes (colour indicates field perturbation amplitude); n=1 and n=2 amplitudes deduced from spectrogram. Edge D_α indicates ELMs and back transition to L mode.

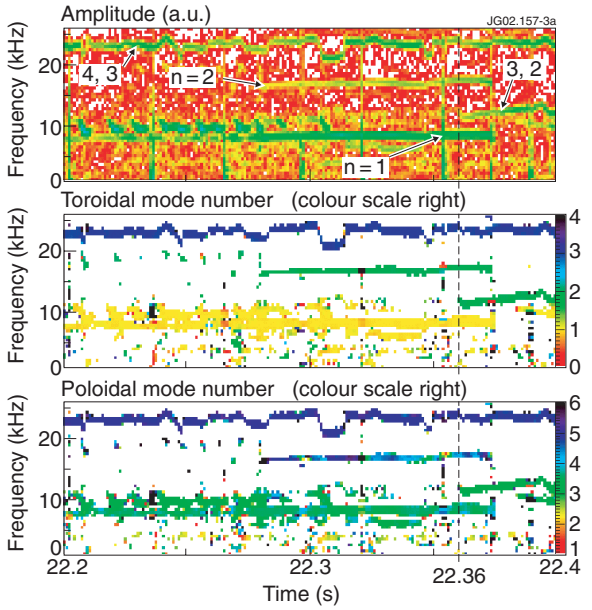

Figure 3a: Onset of (3,2) neoclassical tearing mode in pulse 47285 on JET: spectrograms (frequency vs time) where colour indicates mode amplitude (upper plot), toroidal mode number (middle plot) and poloidal mode number (lower plot), with colour scales indicated to the right of each plot.

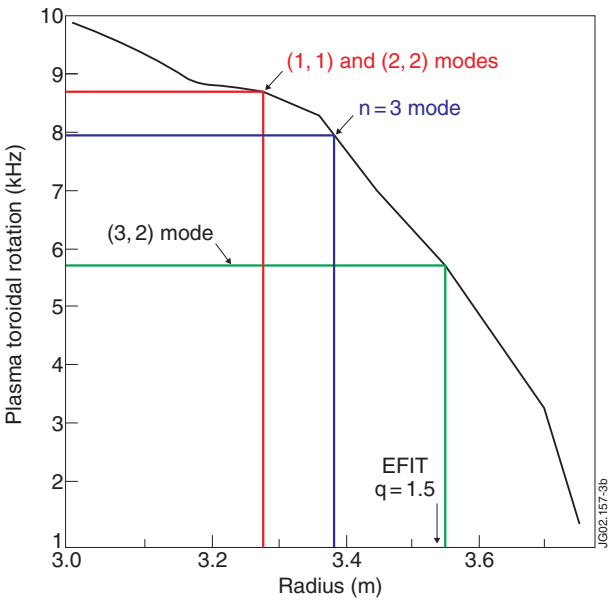

Figure 3b: Charge exchange measurement of plasma toroidal rotation for 47285 at 62.36s (NTM onset), used to identify locations of various modes.

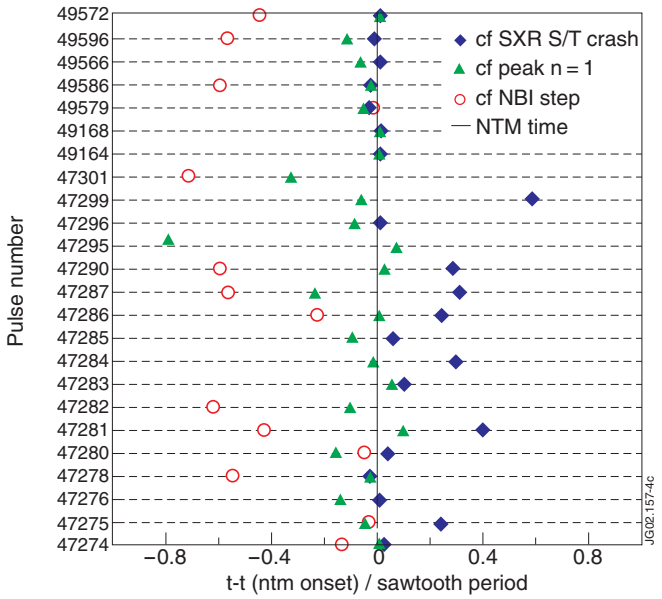

Figure 4: Correlation of (3,2) NTM onset and sawtooth crash or peak in sawtooth MHD, normalised to sawtooth period for 24 pulses.

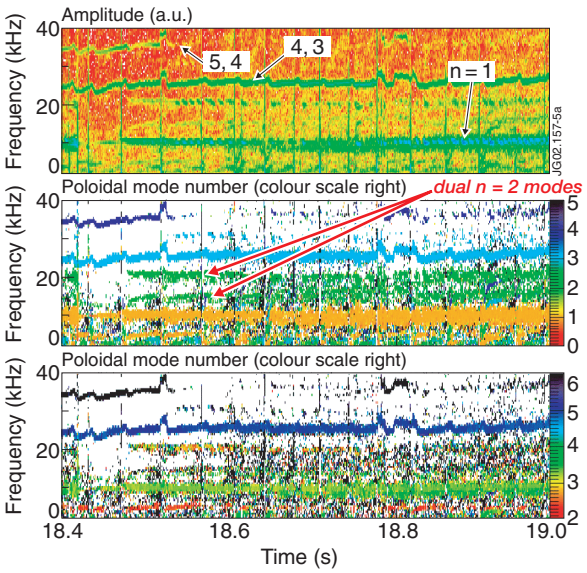

Figure 5a: Prolonged precursor modes in pulse 47277 (plot type as described for Figure 3a).

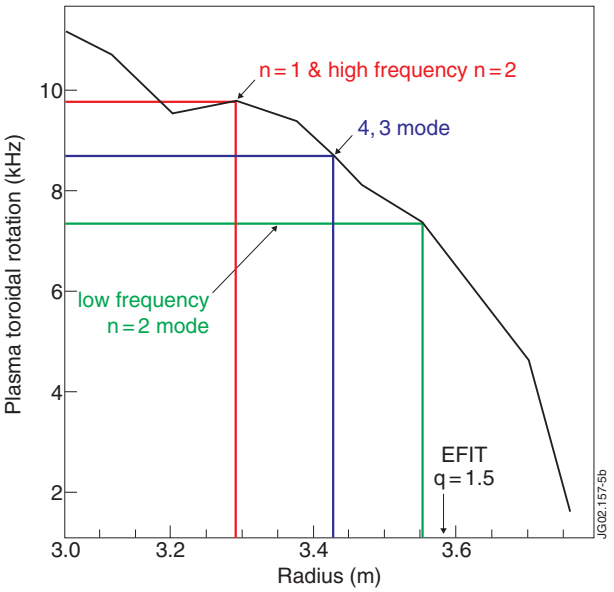

Figure 5b: Charge exchange measurement of plasma toroidal rotation for Figure 5a, used to identify locations of the various modes.

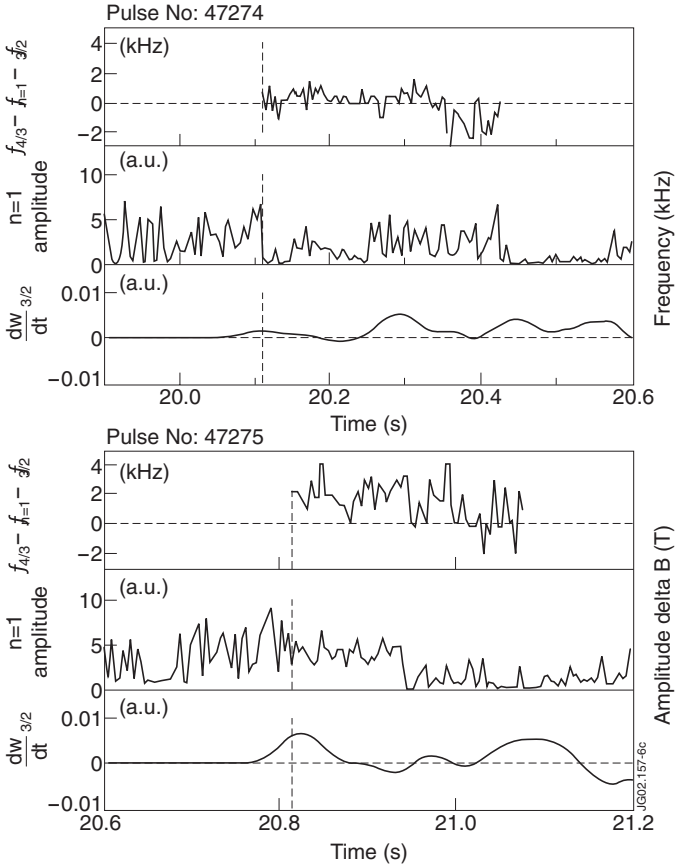

Figure 6: Comparison of three-wave frequency matching condition (upper plot) and n=1 amplitude (middle plot) with smoothed (3,2) NTM island growth rate (lower plot) for two typical discharges: (a) 47274; (b) 47275. Vertical dashed line indicates NTM onset time (dw/dt rise earlier due to smoothing).

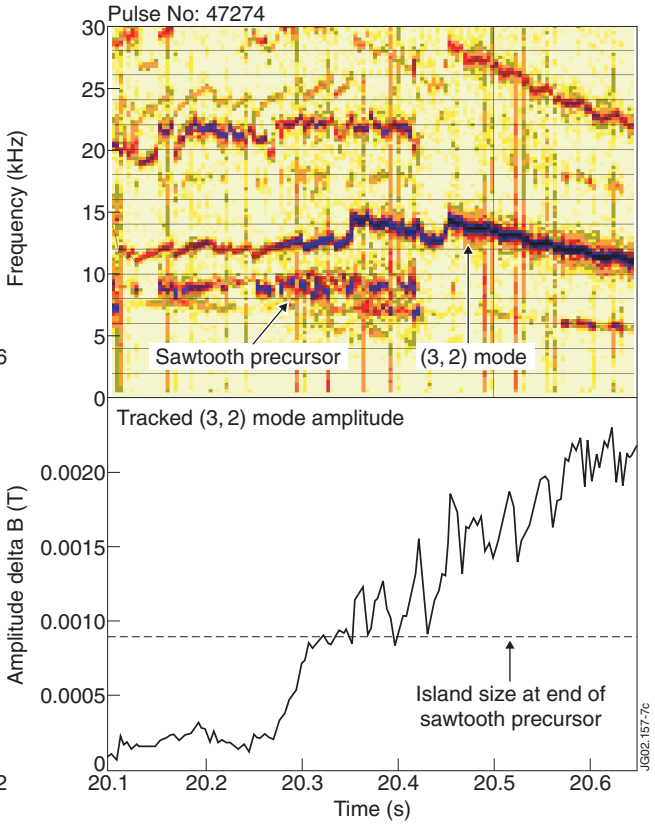

Figure 7: Amplitude of the (3,2) mode during onset of an NTM in pulse 47274.

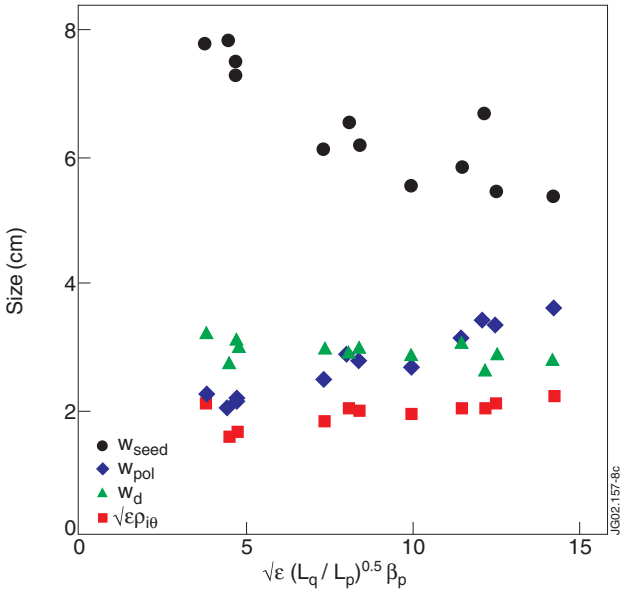

Figure 8: Island sizes at the end of sawtooth precursor phase, and compared with scale lengths for small island size stabilisation terms.

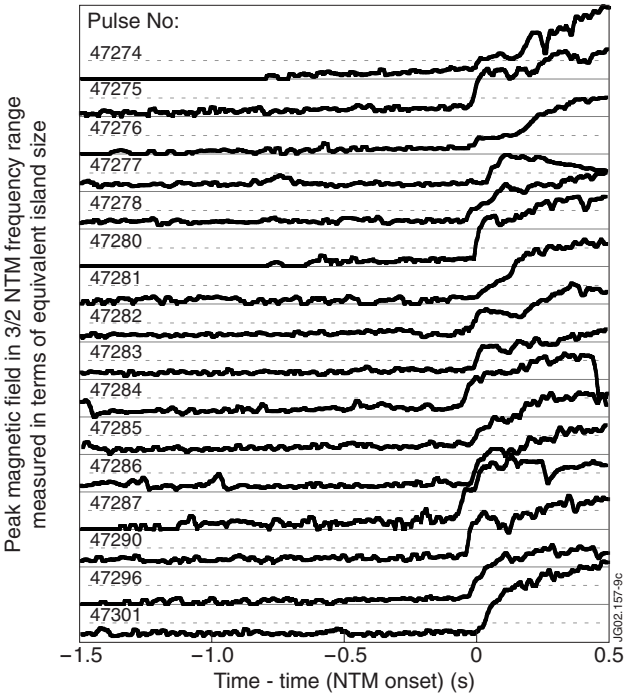

Figure 9: Size of peak magnetic amplitude in the frequency range of the (3,2) NTM prior to and during NTM onset for each of 16 pulses. Amplitude (y value) is measured in terms of the equivalent (3,2) island size. Traces are vertically offset by 6cm with respect to each other, with solid lines indicating zero levels, and dotted lines indicating 3cm island size.

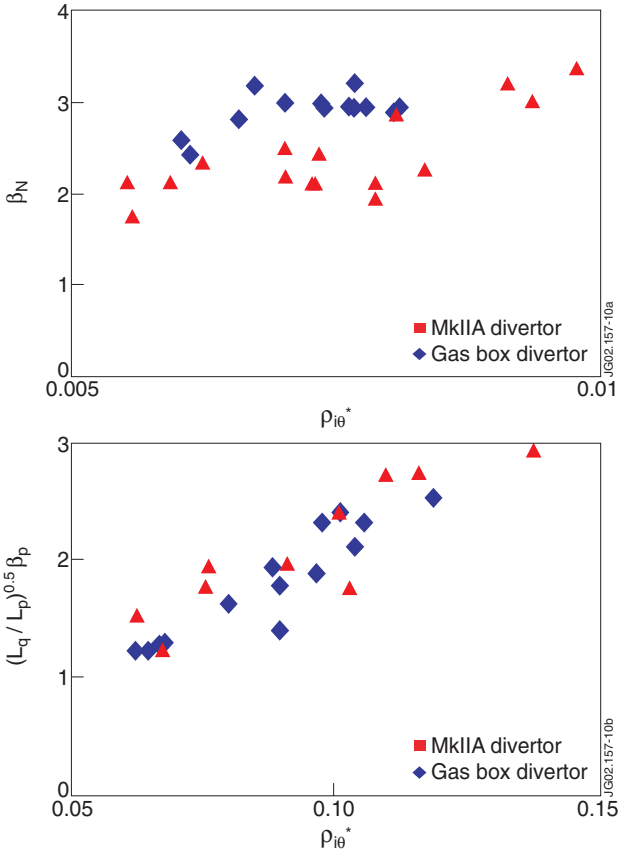

Figure 10a: Best fit for (3,2) NTM onset scaling as 'global' β_N parameter versus $\rho_{i\phi}^*$. Figure 10b: Best fit for (3,2) NTM onset scaling in local 'physics' parameters, corrected for the observed collisionality dependence

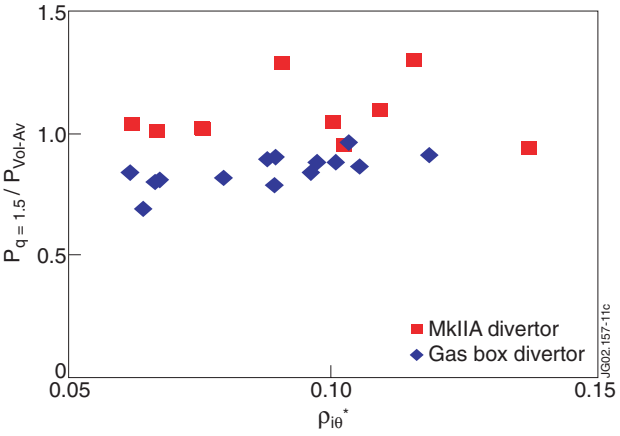

Figure 11: Comparison of pressure at NTM surface to volume average pressure (versus $\rho_{i\theta}^*$) for NTM onset times in two divertor configurations.

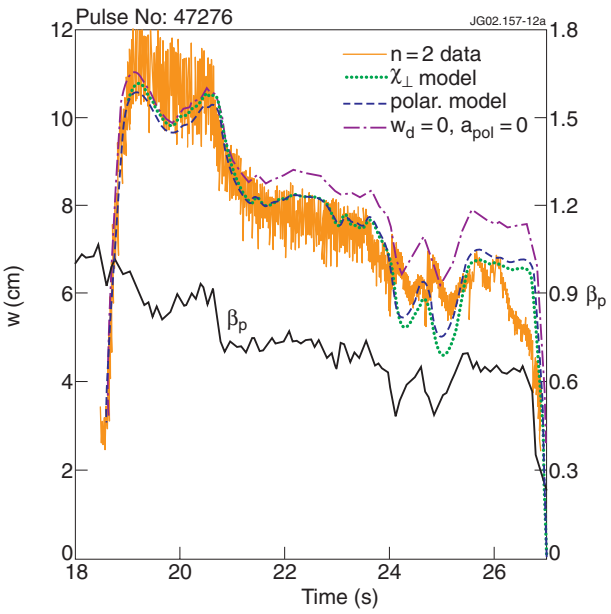

Figure 12a: Comparison of island amplitude evolution (thin line, left scale) with modified Rutherford equation for 47276 with no stabilising terms (dot-dash), ion polarisation term (dash), or island transport terms (dotted) included. A step down in heating results in a fall β_p (lower solid line, right scale), which cannot be matched without stabilising terms.

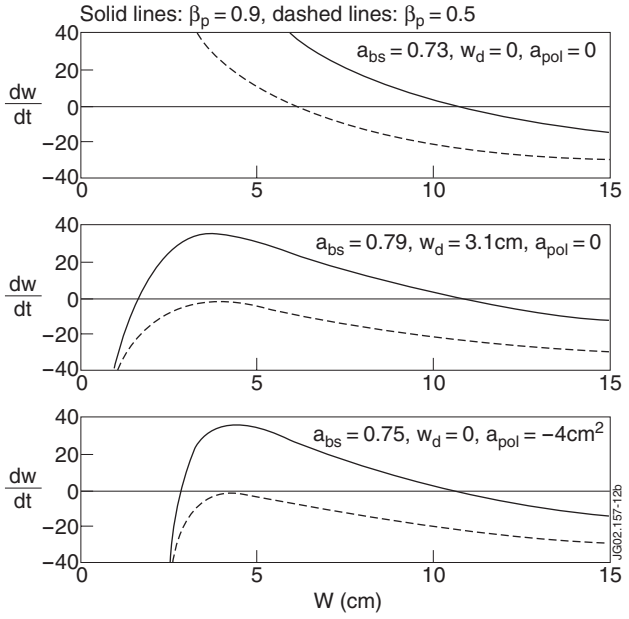

Figure 12b: Growth rates versus island size for three fit models shown in Figure 12a at two β_p values, with fit parameters given

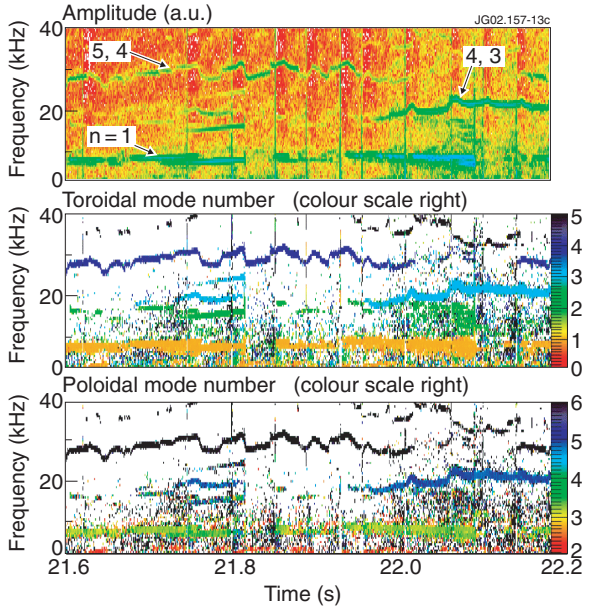

Figure 13: Amplitude and mode number spectrograms for onset of a (4,3) NTM (pulse 47283)

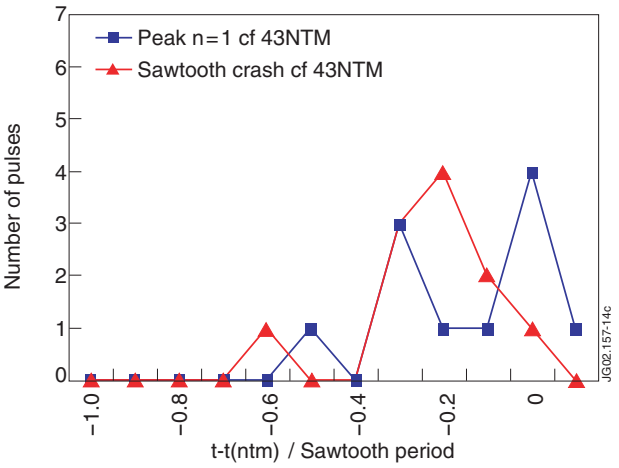

Figure 14: Correlation of (4,3) NTM onset time with sawtooth activity: pulses are binned according to time of NTM relative to sawtooth.

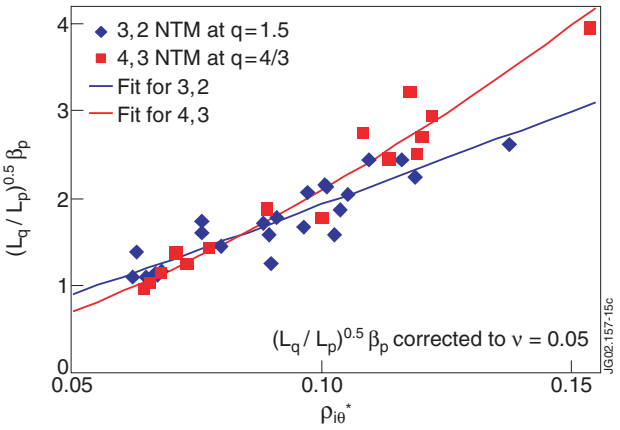

Figure 15: Scaling of (4,3) and (3,2) NTM onset thresholds in terms of local parameters, corrected for collisionality variation.